BIOCHEMISTRY
including biophysical chemistry & molecular biology

Article

pubs.acs.org/biochemistry

Activity and Crystal Structure of *Arabidopsis thaliana* UDP-*N*-Acetylglucosamine Acyltransferase

Sang Hoon Joo,[†] Hak Suk Chung,[‡] Christian R. H. Raetz,[‡] and Teresa A. Garrett*[,§]

[†]Department of Pharmacy, Catholic University of Daegu, Gyeongbuk 712-702, South Korea

[‡]Department of Biochemistry, Duke University Medical Center, Durham, North Carolina 27710, United States

[§]Department of Chemistry, Vassar College, Poughkeepsie, New York 12569, United States

Supporting Information

ABSTRACT: The UDP-*N*-acetylglucosamine (UDP-GlcNAc) acyltransferase, encoded by *lpxA*, catalyzes the first step of lipid A biosynthesis in Gram-negative bacteria, the (*R*)-3-hydroxyacyl-ACP-dependent acylation of the 3-OH group of UDP-GlcNAc. Recently, we demonstrated that the *Arabidopsis thaliana* orthologs of six enzymes of the bacterial lipid A pathway produce lipid A precursors with structures similar to those of *Escherichia coli* lipid A precursors [Li, C., et al. (2011) *Proc. Natl. Acad. Sci. U.S.A. 108*, 11387−11392]. To build upon this finding, we have cloned, purified, and determined the crystal structure of the *A. thaliana* LpxA ortholog (AtLpxA) to 2.1 Å resolution. The overall structure of AtLpxA is very similar to that of *E. coli* LpxA (EcLpxA) with an α-helical-rich C-terminus and characteristic N-terminal left-handed parallel β-helix (LβH). All key catalytic and chain length-determining residues of EcLpxA are conserved in AtLpxA; however, AtLpxA has an additional coil and loop added to the LβH not seen in EcLpxA. Consistent with the similarities between the two structures, purified AtLpxA catalyzes the same reaction as EcLpxA. In addition, *A. thaliana lpxA* complements an *E. coli* mutant lacking the chromosomal *lpxA* and promotes the synthesis of lipid A in vivo similar to the lipid A produced in the presence of *E. coli lpxA*. This work shows that AtLpxA is a functional UDP-GlcNAc acyltransferase that is able to catalyze the same reaction as EcLpxA and supports the hypothesis that lipid A molecules are biosynthesized in *Arabidopsis* and other plants.

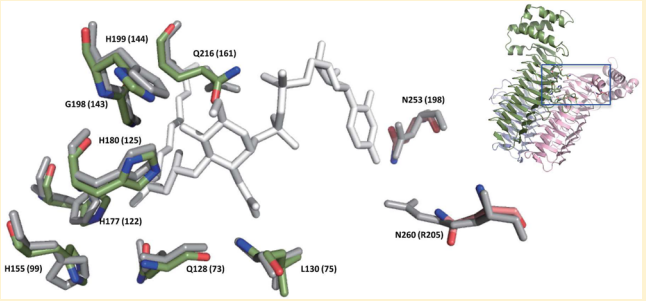

Lipid A is a glucosamine-based phospholipid that anchors lipopolysaccharide (LPS) to the outer monolayer of the outer membrane of Gram-negative bacteria.[1] The synthesis of lipid A in most Gram-negative bacteria is essential for survival, making it a target for antibacterial drugs that combat Gram-negative bacterial infections. The structure of the Kdo_2−lipid A portion of LPS is relatively conserved, and most Gram-negative bacteria encode single-copy homologues of the nine *Escherichia coli* enzymes that catalyze the biosynthesis of the Kdo_2−lipid A moiety.[1]

While Gram-positive bacteria, archaea, fungi, insects, worms, and vertebrates do not contain any of the genes for lipid A synthesis, the majority of higher plants, including *Arabidopsis thaliana*, encode full-length nuclear orthologs of six of the nine key enzymes of the *E. coli* system responsible for the biosynthesis of the Kdo_2−lipid A moiety.[2] The *lpx* genes of *A. thaliana* are functional.[2] When RNAi or chromosomal knockout inactivates the *lpx* genes, the expected lipid A-like precursors are detectable and accumulate as predicted in the total lipid fraction when analyzed by mass spectrometry. Currently, neither the structure nor the function of the lipid A-like molecules generated by plants is known. Considering the low level of lipid A intermediates observed in plants (<0.01% of the total lipid), these molecules may play a role in signal transduction or regulation of the immune response.[2]

In Gram-negative bacteria, the UDP-*N*-acetylglucosamine (UDP-GlcNAc) acyltransferase, LpxA, catalyzes the first step in lipid A biosynthesis (Figure 1),[3] and in most systems, this gene is required for growth.[4] In *E. coli*, LpxA mediates the reversible transfer of the (*R*)-3-hydroxymyristoyl moiety from (*R*)-3-hydroxymyristoyl-acyl carrier protein (ACP) to the glucosamine 3-OH group of UDP-GlcNAc (Figure 1). UDP-GlcNAc acyltransferases, such as LpxA, are soluble cytoplasmic proteins, and they usually require (*R*)-hydroxyacyl-ACPs as donor substrates.[5] LpxAs from different bacteria share a high degree of sequence homology but can show different acyl chain and sugar selectivity. For example, *E. coli* LpxA (EcLpxA) prefers (*R*)-3-hydroxymyristoyl-ACP; *Chlamydia trachomatis* LpxA prefers myristoyl-ACP,[6] and *Helicobacter pylori* LpxA (HpLpxA) prefers (*R*)-3-hydroxypalmitoyl-ACP.[7] *Leptospira interrogans* LpxA uses UDP-2-acetamido-3-amino-2,3-dideoxy-α-D-glucopyranose as a substrate.[8]

Received: February 17, 2012
Revised: April 29, 2012
Published: April 30, 2012

   dx.doi.org/10.1021/bi3002242 | *Biochemistry* 2012, 51, 4322−4330

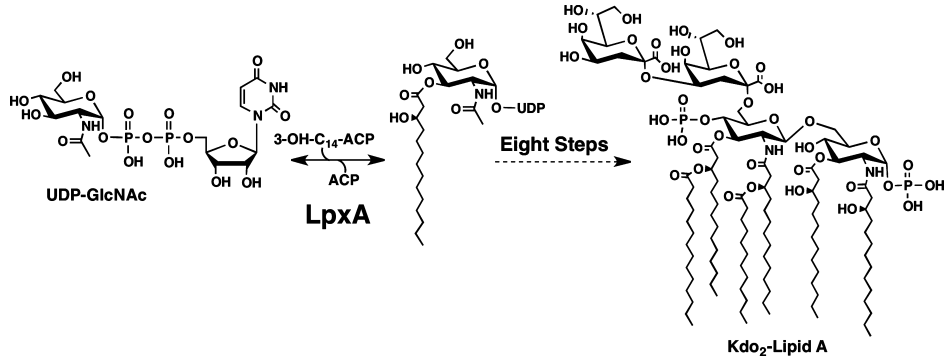

Figure 1. Reaction catalyzed by LpxA. Both EcLpxA and AtLpxA catalyze the acylation of UDP-GlcNAc, the first step in the biosynthesis of the Kdo_2–lipid A moiety. *A. thaliana* has orthologs of six of the nine enyzmes required to biosynthesize the Kdo_2–lipid A moiety in *E. coli*.[2]

A. thaliana LpxA (AtLpxA) and EcLpxA share a significant degree of sequence homology. The initial sequence alignment of the two proteins with ClustalW[9] showed sequences that are 38% identical and 53% similar, with six gaps over 293 amino acid residues (Figure S1 of the Supporting Information). Among the six gaps in the alignment, two are located in the left-handed parallel β-helix (LβH) region,[10] suggesting the existence of two extra inserts in addition to the two loops found in bacterial LpxAs. The first gap consisted of 18 amino acid residues (Asn73–Gly90), and the second gap consisted of four amino acid residues (Glu104–Gly107) (Figure S1 of the Supporting Information). On the basis of this sequence alignment, which suggested a structural deviation from the bacterial LpxA structures determined so far,[7,8,11] we investigated the biochemical properties of AtLpxA in vitro and in vivo and determined its crystal structure to 2.1 Å resolution.

EXPERIMENTAL PROCEDURES

Materials. [α-^{32}P]UTP was purchased from PerkinElmer (Waltham, MA). Oligonucleotide primers were obtained from Integrated DNA Technologies (Coralville, IA). Unless stated otherwise, all enzymes for cloning were from New England Biolabs (Ipswich, MA), and the *E. coli* strain for cloning was XL1-Blue (Table 1) (Stratagene, Cedar Creek, TX). The crystallography reagents, Crystal screen HT, ammonium sulfate, lithium sulfate, and the StockOptions sodium citrate buffer kit, were from Hampton Research (Aliso Viejo, CA). Reactive Green 19 agarose beads were from Sigma (St. Louis, MO). All other chemicals were obtained from VWR (Radnor, PA) or prepared as described below.

Plasmid Construction and Molecular Biology Techniques. The *AtlpxA* gene, excluding the region encoding the predicted signal peptide (residues 2–32),[12] was amplified by polymerization chain reaction (PCR) from a cDNA library of *A. thaliana* (var. Columbia) with primers SJP-017F and SJP-017B (Table 2). The PCR product was digested with restriction enzymes *Nde*I and *Bam*HI and gel purified from a 1% agarose gel using the QIAquick Gel Extraction Kit from Qiagen (Valencia, CA). The digested and gel-purified fragment was ligated into similarly digested pET-21b(+) that was treated with calf intestinal phosphatase to construct SJD-01 (Table 1). The *AtlpxA* gene was subcloned from SJD-01 into pBAD33[13] using the *Xba*I and *Hin*dIII sites to construct pAtLpxA. pHpLpxA (pBAD33 harboring *H. pylori lpxA*) was prepared by subcloning from pCS92, the pET-23 vector containing *HplpxA* (kind gift of C. Sweet, United States Naval Academy, Annapolis, MD), using the *Xba*I and *Hin*dIII sites. Plasmids were isolated with the QIAprep Miniprep kit from Qiagen, and the bacterial genomic DNAs were purified with the Easy-DNA kit from Invitrogen (Carlsbad, CA). All DNA constructs were confirmed by dideoxy sequencing at the DNA Analysis Facility of Duke University.

Table 1. Bacterial Strains and Plasmids

	description	source or reference
	E. coli Strains	
W3110	wild type, F^-, λ^-	*E. coli* Genetic Stock Center (Yale University, New Haven, CT)
DY330	W3110 Δ*lacU169 gal490 λcI857* Δ(*cro-bioA*)	20
XL1-Blue	Δ*mcr ABC recA1 endA1 gyrA96 relA1 supE44 thi-1 lac*	Stratagene
C41(DE3)	*F ompT hsdS*$_B$ ($r_B^-m_B^-$) *gal dcm* (*DE3*) *D* (*srl-recA*)*306::Tn10*	16
SJS-1D	DY330 (*lpxA::kan*)/pHpLpxA	this work
SJS-2W	W3110 (*lpxA::kan*)/pAtLpxA	this work
SM101	*thr-1 araC14 lpxA2*(*ts*) *tsx-78* Δ(*galK-attLAM*)*99 hisG4*(*Oc*) *rfbC1 rpsL136*(*strR*) *xylA5 mtl-1 thi-1*	4
	Plasmids	
pET-21b(+)	expression vector containing a T7 promoter, Amp^R	EMD Chemicals
pET-30a(+)	expression vector containing a T7 promoter, Cam^R	EMD Chemicals
pBAD33	medium-copy vector, Cam^R	13
pCS92	expression vector pET-23c(+) containing HpLpxA, Amp^R	C. Sweet
SJD-01	pET-21b(+) containing AtLpxA	this work
pHpLpxA	pBAD33 containing HpLpxA	this work
pAtLpxA	pBAD33 containing AtLpxA	this work

AtLpxA Expression and Purification. The AtLpxA protein was overexpressed and purified by modifying the previously described method for the purification of EcLpxA.[14,15] *E. coli* C41(DE3) cells[16] harboring SJD-01 were grown overnight in LB medium[17] supplemented with 100 μg/mL ampicillin at 37 °C while being shaken at 220 rpm. The overnight culture was diluted ~100-fold into fresh LB medium containing 100 μg/mL ampicillin and grown to an A_{600} of ~0.6 at 37 °C. Protein expression was induced for 4 h with 0.2 mM isopropyl β-D-thiogalactopyranoside at 37 °C (Figure S2A of the Supporting Information). Cells from a 1 L culture were harvested by centrifugation for 15 min at 4 °C and 4000*g* and washed with phosphate-buffered saline (PBS) (137 mM NaCl, 2.7 mM KCl, 10 mM Na_2HPO_4, and 2 mM KH_2PO_4). The cell pellet was resuspended in 20 mL of ice-cold lysis buffer

dx.doi.org/10.1021/bi3002242 | *Biochemistry* 2012, 51, 4322–4330

Table 2. Oligonucleotide Primers Used in This Study

	SJD-01[a]
SJP-017F	5′-gagatatacatATGGATTCGAGGGATTCTGAAGTCTTAATACACC-3′
SJP-017B	5′-cgaattcggatccTAAGTTGTGGAATCGAGCCATTGTCTG-3′
	kan Cassette[b]
SJP-030F	5′-GCGAAGCAACGATGATGTGTGCTCGTAGCCGGGAGGCCTGA tac ATGAGCCATATTCAACGGGAAACGTCTTG-3′
SJP-030B	5′-CGGCGACCAGGGCAATCGTTAATGGACGCTGTTCAGTCAT ggtatat **ctcctt** TTAGAAAAACTCATCGAGCATCAAATGAAAC-3′
	∼100 bp above and below the *lpxA* Open Reading Frame Region in the *E. coli* Chromosome
SJP-028F	5′-CGCCGCGGCCTGACC-3′
SJP-028B	5′-CGTGGCCCGGCAACACCAAC-3′
	Inside the *kan* Cassette
SJP-029F	5′-AATATTGTTGATGCGCTGGC-3′
SJP-029B	5′-AGCGAGACGAAATACGCGA-3′
	Sequencing Primer
T7P	5′-TAATACGACTCACTATAGGG-3′
T7T	5′-GCTAGTTATTGCTCAGCGG-3′
pBAD-F	5′-ATGCCATAGCATTTTTATCC-3′
pBAD-B	5′-GATTTAATCTGTATCAGG-3′

[a]Open reading frames are capitalized, and the restriction sites, *Nde*I (CATATG) and *Bam*HI (GGATCC), are underlined. [b]Open reading frames are capitalized; *kan* is underlined, and *lpxB* is italic and underlined. The ribosome binding site (bold) was inserted during primer design for *lpxB*[36] expression.

[10 mM potassium phosphate buffer (pH 7.0) and 20% glycerol]. The cells were disrupted by one passage through a French pressure cell at 18000 psi. The suspension of lysed cells was centrifuged at 4 °C and 140000*g* for 1 h to remove unlysed cells and cell membranes. The supernatant (∼20 mL, ∼180 mg of total protein) was loaded onto a Reactive Green-19 Agarose column (25 mL bed volume), pre-equilibrated with lysis buffer. After the column had been washed with 50 mL of lysis buffer, the bound proteins were eluted with 50−100 mL each of lysis buffer containing 100 mM, 200 mM, 400 mM, and 1 M KCl. Each fraction was analyzed via SDS−PAGE to determine the fractions containing AtLpxA (Figure S2B of the Supporting Information). The fractions containing AtLpxA (four fractions totaling ∼200 mL) were pooled and concentrated to approximately 20 mL (∼1 mg/mL) with an Amicon stirred cell concentrator (Millipore, Billerica, MA). A portion (10 mL) was loaded onto a HiLoad 26/60 Superdex 200 prep grade column (320 mL bed volume, GE Healthcare), pre-equilibrated with 10 mM potassium phosphate buffer (pH 7.0) containing 200 mM KCl and 20% glycerol. Fractions containing AtLpxA (Figure S2B of the Supporting Information) were pooled and concentrated to ∼18 mg/mL for storage. The concentration of protein was determined by both the absorbance at 280 nm and the BCA assay kit (Pierce, Rockford, IL). The purity of the protein was evaluated by SDS−PAGE. The purified protein was flash-frozen in liquid nitrogen and stored at −80 °C.

LpxA Activity Assays. (*R*,*S*)-3-Hydroxymyristoyl-ACP was obtained as described previously,[18,19] and the LpxA assay conditions were similar to those reported previously[14,15] with minor modifications. Each reaction mixture (typically 10 μL) contained 40 mM Hepes (pH 7.4), 1 mg/mL bovine serum albumin, 10 μM (*R*,*S*)-3-hydroxymyristoyl-ACP, and 10 μM [α-^{32}P]UDP-GlcNAc at 9 × 10^5 μCi/mmol. The reaction was started by the addition of enzyme (typically 0.5−20 μg/mL) and the mixture incubated at 30 °C for the times indicated. The reactions were terminated by spotting 1 μL portions onto a 0.25 mm silica gel 60 thin layer chromatography plate (EMD Chemicals, Gibbstown, NJ). The plates were developed in a $CHCl_3$/CH_3OH/H_2O/CH_3COOH mixture (25:15:4:2, v/v/v/v). The plate was exposed to a PhosphorImager screen overnight, and the extent of acylation of [α-^{32}P]UDP-GlcNAc was determined by scanning with a Storm 840 PhosphorImager (GE Healthcare, Piscataway, NJ).

Construction of a Conditional *lpxA* Chromosomal Knockout Strain. To construct a conditional *lpxA* chromosomal knockout strain, we replaced the *E. coli* chromosomal copy of *lpxA* with a kanamycin resistance cassette in the presence of an appropriate covering plasmid, pHpLpxA or pAtLpxA (Table 1). The kanamycin resistance cassette (*kan*) was amplified from plasmid pET30a(+) (EMD Chemicals) with primers SJP-030F and SJP-030B (Table 2), using KOD hot start DNA polymerase following the manufacturer's protocol (EMD Chemicals). In addition to sequences homologous to the *kan* gene, primer SJP-030F contains 44 bp of genomic DNA upstream of the 5′ end of *lpxA* and primer SJP-030B contains a ribosome binding site followed by the first 34 bp of the downstream *lpxB* gene on the 3′ end. The resulting PCR product was resolved on a 1% agarose gel and purified with the QIAquick gel extraction kit from Qiagen.

The initial conditional mutant was constructed using the *E. coli* DY330 strain (Table 1) that carries the λ RED recombinase[20] and pHpLpxA. Electrocompetent DY330/pHpLpxA cells were prepared by a published protocol.[21] Briefly, DY330/pHpLpxA cells were grown at 30 °C in 50 mL of LB medium containing 25 μg/mL chloramphenicol and 0.2% L-arabinose until the A_{600} of the cells reached ∼0.4. Then the culture was shifted to 42 °C for 15 min to activate the λ RED genes.[20] Next, the cells were washed twice with 30 mL of ice-cold water and then resuspended in 500 μL of ice-cold water. A portion of cells (100 μL) was used for electroporation with the *lpxA::kan* PCR product generated as described above. Following electroporation, the cells were grown for 2 h at 30 °C in 1 mL of LB medium containing 0.2% L-arabinose. The cells were harvested and resuspended in a final volume of 100 μL of LB medium and then plated onto LB-agar plates, containing 0.2% L-arabinose, 25 μg/mL chloramphenicol, and 20 μg/mL kanamycin (LB-ara-cam-kan). The plate was incubated at 30 °C overnight. The resulting colonies were repurified by being streaked on LB-ara-cam-kan. To confirm chromosomal *lpxA* deletion, the *lpxA* region on the chromosome of DY330

lpxA::kan/pHpLpxA was amplified with primers SJP-028F and SJP-028B (see Table 2 and Figure S3B of the Supporting Information) and sequenced with primer SJP-028F at the Duke University DNA Analysis Facility. The resulting strain was named SJS-1D (Table 1).

A P1 lysate was prepared from SJS-1D to transduce *lpxA::kan* into the *E. coli* W3110 cells harboring pAtLpxA (pBAD33 carrying AtLpxA) or pBAD33 as a control. W3110 *lpxA::kan* pAtLpxA was selected and purified twice from a LB-ara-cam-kan plate containing 100 mM sodium citrate and named SJS-2W (Table 1). Consistent with *lpxA* being required for growth,[4] transductants were only viable with cells harboring pAtLpxA and not with cells containing the control vector pBAD33. For in vivo complementation tests, SJS-2W and W3110/pBAD33 cells were streaked on the LB-cam plates containing 0, 0.02, or 0.2% L-arabinose.

Isolation and Characterization of Lipid A Species. An overnight culture of *E. coli* SJS-2W cells and W3110/pBAD33 were grown at 37 °C and diluted ~100-fold in fresh LB medium supplemented with 25 μg/mL chloramphenicol and 0.2% L-arabinose. Cells were grown at 37 °C while being shaken at 220 rpm until the A_{600} reached ~1.0. Cells from a 200 mL culture were harvested by centrifugation at 4 °C and 4000*g* and washed with 50 mL of PBS. The cell pellet was resuspended in 20 mL of PBS, and then 50 mL of CH_3OH and 25 mL of $CHCl_3$ were added to generate a single-phase Bligh−Dyer extraction mixture (1:2:0.8 $CHCl_3$/CH_3OH/PBS, v/v/v).[22] The single-phase mixture was incubated at room temperature while being stirred for 1 h. The pellet was recovered by centrifugation at room temperature and 2500*g* for 20 min, and the pellet was washed again with 40 mL of a $CHCl_3$/CH_3OH/PBS mixture (1:2:0.8, v/v/v). The pellet was air-dried and then resuspended in 25 mL of 50 mM sodium acetate. The pH of the suspension was adjusted to 4.5 via addition of 2−3 drops of glacial acetic acid. The suspension was then incubated at 100 °C for 30 min to hydrolyze the Kdo−lipid A linkage.[23] The hydrolysis mixture was cooled to room temperature, and then CH_3OH and $CHCl_3$ (28 mL each) were added to form a two-phase Bligh−Dyer mixture.[22] The lipid A extracted into the lower phase was collected and concentrated with a rotary evaporator. The dried sample was dissolved in a $CHCl_3$/CH_3OH mixture (2:1, v/v) and then subjected to mass spectrometry analysis using a QSTAR XL electrospray ionization quadrupole time-of-flight mass spectrometer (Applied Biosystems, Foster City, CA) in negative-ion mode as described previously.[24,25] Data analysis was conducted with the Analyst QS software suite (Applied Biosystems). Exact masses were determined using ChemBioDraw Ultra version 12.0.3.

Crystallization and Structure Determination. Initial crystals of AtLpxA were found by screening against the Crystal Screen HT matrix (Hampton Research) using the sitting-drop vapor diffusion method with the Phoenix RE robotics system (Art Robbins Instruments, Sunnyvale, CA). Purified AtLpxA [18 mg/mL in 10 mM potassium phosphate buffer (pH 7.0), 200 mM KCl, and 20% glycerol] was mixed in a 1:1 ratio with a precipitant solution containing 0.5 M ammonium sulfate, 0.1 M sodium citrate tribasic dihydrate (pH 5.6), and 1.0 M lithium sulfate monohydrate and allowed to equilibrate at 20 °C. Hexagonal-shaped crystals appeared after 1−2 days and grew to a maximal size of ~60 μm × 60 μm × 25 μm. Crystals were frozen in liquid N_2. X-ray diffraction data were collected on SER-CAT beamline 22-BM at the Advanced Photon Source (APS) at Argonne National Laboratory (Argonne, IL). The data were processed and scaled using HKL2000[26] (Table 3).

Table 3. Data Collection and Refinement Statistics for AtLpxA

Data Collection[a]	
source/detector	SER-CAT 22-BM/Mar225 CCD
space group	$P6_322$
a, *b*, *c* (Å)	86.2, 86.2, 200.3
wavelength (Å)	1.00
oscillation range/Δ (deg)	0−90/0.75
resolution (Å)	50.00−2.10 (2.14−2.10)
no. of reflections	
measured	663184
unique	26374
completeness (%)	100.0 (100.0)
average $I/\sigma(I)$	21.4 (3.1)
redundancy	10.5 (9.1)
R_{merge} (%)	11.0 (55.0)
Refinement	
resolution (Å)	24.88−2.10 (2.16−2.10)
no. of reflections	24836
R_{work} (%)	20.7
R_{free} (%)[b]	24.1
rmsd	
bond lengths (Å)	0.009
bond angles (deg)	1.163
no. of protein residues in the asymmetric unit	288
no. of water molecules	165
average *B* factor (Å^2)	
protein	18.0
water	25.9
Ramachandran (%)	
favored regions	96.15
allowed regions	99.65
disallowed regions	0.35
all-atom clash score	6.95
MolProbity score	1.64

[a]Data for the highest-resolution shell are given in parentheses. Data were collected from a single crystal. [b]R_{free} is the *R* value obtained for a test set of reflections consisting of a randomly selected 5% subset for the data excluded from refinement.

The structure of AtLpxA was determined by the molecular replacement method using PHASER[27,28] and a polyalanine search model prepared from the coordinates of LpxA from *E. coli* [Protein Data Bank (PDB) entry 1LXA].[10] Regions outside the hexapeptide repeats were removed from the initial MR solution and manually rebuilt using COOT.[29] Iterative restrained refinement was conducted using REFMAC5[30] within the CCP4 software suite[31] with TLSMD options selected.[32] The final model yielded an R_{work} of 20.7% and an R_{free} of 24.1% and was validated using MOLPROBITY,[33] which reported 96.15% of the residues in the Ramachandran favored region and 0.35% in the outlier region. The data statistics are summarized in Table 3. Secondary structure elements were analyzed with the help of STRIDE,[34] along with a comparison to the known structures of LpxA from several bacteria. Structural alignments and figures were prepared using PyMol.[35] Atomic coordinates and structure factors for AtLpxA were deposited as PDB entry 3T57.

RESULTS

In Vitro Activity of the AtLpxA Enzyme. AtLpxA was purified to homogeneity (Figure S2B of the Supporting Information)

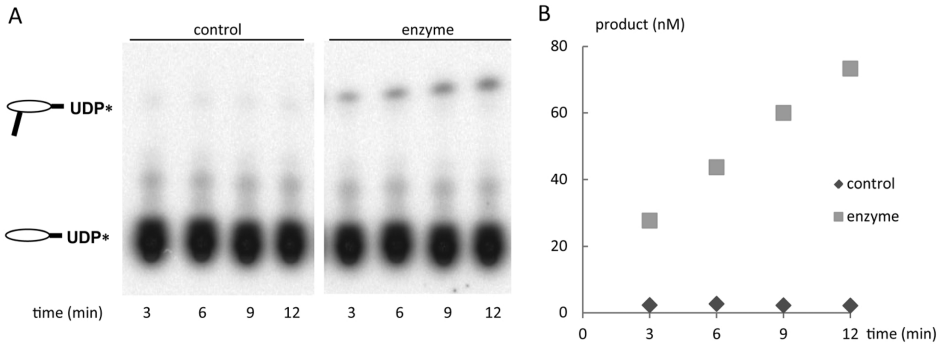

Figure 2. Activity of purified AtLpxA expressed in *E. coli*. Purified AtLpxA (1 μg/mL) was assayed in a reaction mixture containing 40 mM Hepes buffer, radiolabeled UDP-GlcNAc (10 μM), and (*R*,*S*)-3-hydroxymyristoyl-ACP (10 μM) for the time indicated at 30 °C. (A) Reaction products in the presence and absence of AtLpxA after separation using thin layer chromatography. (B) Formation of [α-^{32}P]-UDP-3-*O*-[(*R*)-3-hydroxymyristoyl]-UDP-GlcNAc was quantified with a PhosphorImager as described in Experimental Procedures and plotted vs time.

and was active under in vitro assay conditions for EcLpxA (Figure 2). In vitro assays show AtLpxA transfers a 3-hydroxymyristoyl group from 3-hydroxymyristoyl-ACP to the 3-OH group of UDP-GlcNAc with a specific activity of 5.1 nmol min^{-1} mg^{-1}, ~10 times lower than that of purified EcLpxA when assayed in parallel. While the activity of AtLpxA was lower than that of EcLpxA, it is comparable to the enzymatic activities of other LpxA orthologs from *Francisella novicida* and *H. pylori* purified from the *E. coli* expression system (S. Joo et al., manuscript in preparation).

Complementation of the *E. coli lpxA* Knockout Mutant by *A. thaliana lpxA*. *lpxA* genes from other Gram-negative bacteria are able to rescue the phenotype of a temperature-sensitive mutant of *E. coli lpxA*, SM101.[4,6] However, attempts to complement SM101 with *AtlpxA* were unsuccessful. To test whether *AtlpxA* could functionally replace *EclpxA*, we constructed a conditional mutant with a deletion of the chromosomal copy of *E. coli lpxA*. In this mutant, only *lpxA* provided on the covering plasmid would be expressed preventing the formation of LpxA heterotrimers of EcLpxA and AtLpxA.

A plasmid containing *AtlpxA* under control of an arabinose inducible promoter, pAtLpxA, supported the growth of the *E. coli lpxA::kan* mutant on LB plates but only when *AtlpxA* expression was induced by the presence of L-arabinose (0.02 or 0.2%) (Figure 3). In the absence of L-arabinose, *AtlpxA* expression

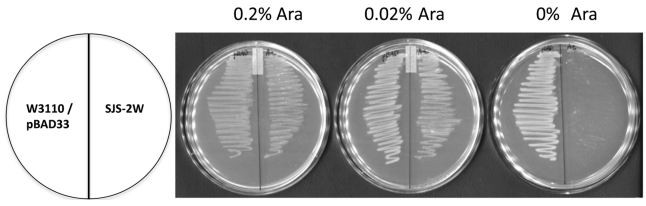

Figure 3. Complementation of *E. coli lpxA::kan* with *AtlpxA*. Cells, W3110/pBAD33 and SJS-2W, were streaked, as indicated by the schematic, onto LB agar plates containing 25 μg/mL chloramphenicol and 0, 0.02, or 0.2% L-arabinose and incubated overnight at 37 °C.

was not induced and the cells did not survive, consistent with *lpxA* being required for growth.[4,6] This result clearly shows that a plant *lpxA* can functionally replace *EclpxA*. Combined with the in vitro assay data described above, it is extremely likely that AtLpxA functions like EcLpxA and may function similarly in *A. thaliana*.

Characterization of Lipid A Species. In addition to possessing in vitro enzyme activity analogous to that of EcLpxA, AtLpxA was able to functionally replace EcLpxA by supporting the biosynthesis of the expected lipid A anchor of LPS. LPS from SJS-2W cells and W3110/pBAD33 was subjected to mild acid hydrolysis to release lipid A for characterization using negative-ion electrospray ionization quadrupole time-of-flight mass spectrometry (ESI-MS). The overall lipid A profiles of SJS-2W, *lpxA::kan* covered by pAtLpxA, and W3110/pBAD33 are remarkably similar. The major negative ions observed are doubly charged $[M - 2H^+]^{2-}$ ions.[24] The $[M - 2H^+]^{2-}$ ion at *m*/*z* 897.70 corresponds to the major hexa-acylated lipid A species (exact mass of *m*/*z* 897.6024) (Figure 4, inset) and is the prominent ion in both spectra. The $[M - 2H^+]^{2-}$ ion at *m*/*z* 883.68 corresponds to the $[M - 2H^+]^{2-}$ ion of a minor species of hexa-acylated lipid A in which one of the six acyl chains is shorter by two methylenes (exact mass of *m*/*z* 883.5867). These shorter chains are likely caused by the lack of acyl chain specificity of one of the late acyl transferases.[24] For example, the secondary 14-carbon myristate chain added by LpxM to the 3′-hydroxymyristate might be replaced with a 12-carbon laurate moiety. The $[M - 2H^+]^{2-}$ ion at *m*/*z* 783.59 corresponds to the loss of the myristate group as a free acid (RCOOH) (exact mass of *m*/*z* 783.4979), likely occurring during the mass spectrometry analysis.[24] The minor $[M - 2H^+]^{2-}$ ion at *m*/*z* 857.72 corresponds to the dephosphorylated lipid A species (exact mass of *m*/*z* 857.6195) that is likely produced during mild acid hydrolysis of LPS. Taken together, AtLpxA promotes the formation of the same lipid A species in vivo as EcLpxA. These data also provide insight into the acyl chain specificity of AtLpxA. The predominant lipid A formed in the presence of AtLpxA is exactly the same as the lipid A formed by EcLpxA, indicating that AtLpxA has a preference for (*R*)-3-hydroxymyristoyl-ACP like EcLpxA.[5]

Crystal Structure of AtLpxA. On the basis of the high level of sequence identity (38%), conservation of key active site residues, and the in vitro and in vivo activity reported above, AtLpxA appears to be biochemically similar to EcLpxA. To determine how AtLpxA varies structurally from EcLpxA, we investigated the structure of AtLpxA. Like EcLpxA, AtLpxA is a homotrimer in aqueous solution, as judged by size-exclusion chromatography of the catalytically active enzyme (Figure S2B of the Supporting Information). Crystals of AtLpxA were grown and diffracted to 2.1 Å. Similar to EcLpxA,[10] AtLpxA crystallized with a single polypeptide chain in the asymmetric

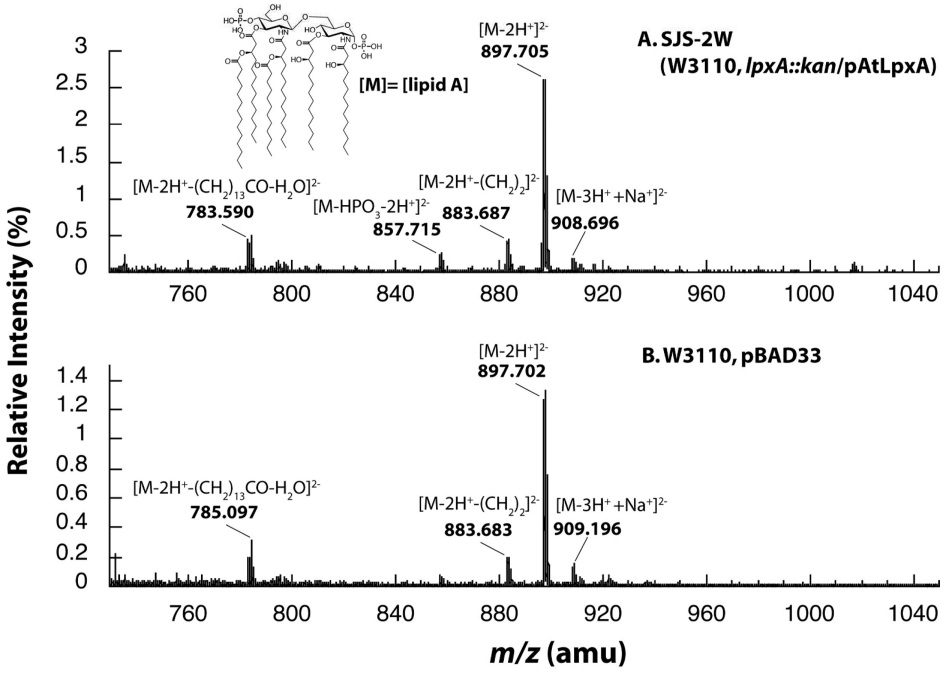

Figure 4. Negative-ion ESI-MS analysis of lipid A species purified from SJS-2W and W3110/pBAD33. Negative-ion ESI-MS from m/z 750 to 1040 of the lipid A species isolated from SJS-2W (A) and W3110/pBAD33 (B). The lipid A species are remarkably similar between the two samples, consistent with AtLpxA and EcLpxA having similar activities in vivo and in vitro. The predominant ions are $[M - 2H]^{2-}$ ions; however, $[M - 3H^+ + Na^+]^{2-}$ ions are also detected at m/z 908.59.

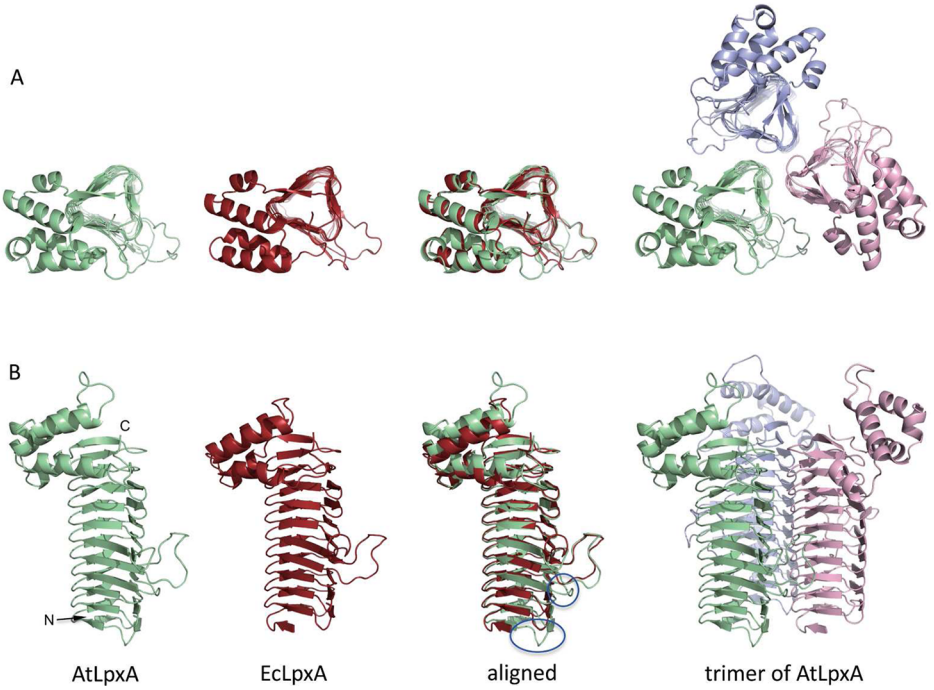

Figure 5. Structure of AtLpxA. (A) Top-down views of the asymmetric units of AtLpxA (green), EcLpxA (red), and the biological trimer of AtLpxA (pale green, light pink, and light blue). (B) Side views of the molecules as indicated. Circled areas correspond to coil C0 and loop 0 of AtLpxA.

unit, and the homotrimer is formed about a crystallographic 3-fold axis of symmetry. Although the majority of AtLpxA could be built, two regions were omitted from the final model because of insufficient, noncontiguous electron density. The first region consists of seven residues (Asp33−Val39) localized to the N-terminus, and the second constitutes nine residues positioned at the C-terminus (Phe328−Thr336).

The overall structure of AtLpxA is similar to the structures of EcLpxA and other LpxA species determined thus far with the characteristic N-terminal LβH domain, in the shape of a triangular prism, connected to the C-terminal portion that is comprised mainly of α-helices (Figure 5).[7,10,11]

The N-terminal LβH domain of the AtLpxA protein (residues Leu40−Met241) consists of 31 β-strands; 29 of

dx.doi.org/10.1021/bi3002242 | Biochemistry 2012, 51, 4322−4330

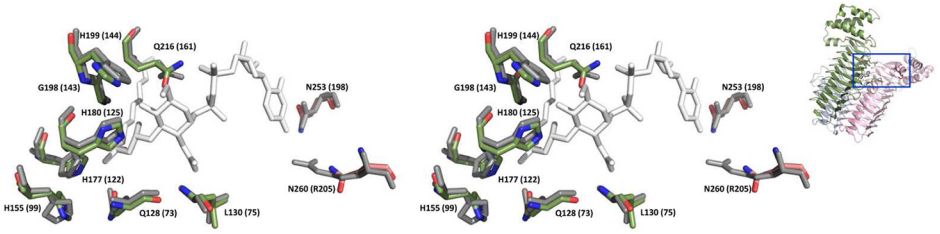

Figure 6. Overlay of the conserved residues within the active site of AtLpxA on that of EcLpxA (stereoview). Residues in the active site of AtLpxA superimposed with the structure of EcLpxA complexed with its product, UDP-3-*O*-[(*R*)-3-hydroxymyristoyl]-GlcNAc (PDB entry 2QIA).[11] Water molecules have been omitted to highlight the conservation of residues between AtLpxA and EcLpxA. AtLpxA residues, EcLpxA residues, and the product are colored green, gray, and white, respectively. The residue names and numbers of AtLpxA are shown, with the corresponding residues from EcLpxA in parentheses. In the inset, the box on the AtLpxA trimer indicates the active site area enlarged in the figure.

these comprise 10 β-helical coils (C1−C10) similar to those found in EcLpxA. Two additional β-strands shape the partial coil C0. As seen in other LpxA proteins, two loops, loop 1, and loop 2, interfere with the LβH domain. Loop 1 is inserted after the fourth coil (C4) and loop 2 after the fifth coil (C5) of AtLpxA. Loop 1 and loop 2 are one amino acid shorter and one amino acid longer, respectively, than the corresponding loops found in EcLpxA but otherwise have conformations similar to those of EcLpxA. In addition to these two loops, the initial sequence alignment predicted two extra loops (Figure S1 of the Supporting Information). Of the two additional loops, the smaller, four-residue loop forms loop 0 (residues Glu104−Gly107) and interrupts the β-helix right after the third helical coil (C3). This small loop contains a Glu104 residue, the OE1 atom of which is 3.9 Å from the hydroxyl oxygen of Tyr78 that belongs to the adjacent monomer. The triangular rod of the LβH domain is bent ~7° in a counterclockwise direction at loop 0, when seen from the amino-terminal side of the 3-fold axis (Figure S4 of the Supporting Information). The larger, 18-residue insert (Asn73−Gly90) predicted from the initial sequence alignments to interrupt the β-helix actually turned out to form a coil of three hexapeptide repeats. These additional hexapeptide repeats result in the extra coil, C0, discussed above.

The C-terminal portion of AtLpxA (residues Val242−Thr336) consists of five α-helices that have slightly different tilts and loops of different lengths as compared to those of EcLpxA but is overall very similar. Superposition of EcLpxA and AtLpxA yielded an rmsd of 0.9 Å for 180 Cα atom pairs, as determined by analysis in PyMol. In addition, key LpxA active site residues[11,15] are similarly positioned when AtLpxA is compared with EcLpxA bound to UDP-3-*O*-[(*R*)-3-hydroxymyristoyl]-GlcNAc[11] (Figure 6).

DISCUSSION

Through the cloning, purification, and crystallization of AtLpxA, we have shown that this plant enzyme shares significant similarities with bacterial EcLpxA. The purified AtLpxA catalyzes the same in vitro reaction, the transfer of an (*R*)-3-hydroxymyristoyl chain from (*R*)-3-hydroxylmyristoyl-ACP to the 3′-hydroxyl of the glucosamine of UDP-GlcNAc. In addition, AtLpxA is able to functionally replace EcLpxA, rescuing an *E. coli lpxA* knockout and promoting the synthesis of *E. coli*-like lipid A in vivo. Altogether, this work clearly supports the hypothesis that plants, such as *A. thaliana*, that possess *lpx* genes synthesize lipid A-like molecules similar to those found in Gram-negative bacteria.

AtLpxA possesses the same in vitro enzyme activity as EcLpxA. While its activity is only one-tenth of that of EcLpxA, this level is similar to that of other LpxA orthologs, such as those from *H. pylori* and *F. novicida* (S. H. Joo et al., manuscript in preparation), expressed and purified using *E. coli* expression systems. It is possible that the lower activity is an inherent property of AtLpxA; however, it is possible that the substrates used in the assay were not optimal for the enzyme. The ACP used in the in vitro assays was from *E. coli*, not *A. thaliana*. The *E. coli* acyl-ACP may not bind as efficiently to AtLpxA, leading to a lower specific activity. Our data and previous results point to a glucosamine-based nucleotide diphosphate being the substrate for AtLpxA; glucosamine-based lipid A-like molecules are detected in *A. thaliana* lipid extracts.[2]

While we have not studied the in vivo substrate specificity of AtLpxA thoroughly, our data support specificity for (*R*)-3-hydroxymyristoyl-ACP over other chain lengths. The lipid A species isolated from SJS-2W, *lpxA::kan* covered by pAtLpxA, was identical to the lipid A profile isolated from wild-type *E. coli*. If AtLpxA preferred other acyl chain lengths, it is likely that it would impact the lipid A species observed in vivo, as observed previously.[6,37]

Previous work has shown that LpxA orthologs can rescue the phenotype of a well-characterized temperature-sensitive *lpxA* mutant, SM101.[4,6] For example, *lpxA* from *H. pylori* supports the growth of *E. coli lpxA* temperature-sensitive mutant SM101 (C. Sweet et al., manuscript in preparation) at 42 °C. AtLpxA did not rescue SM101 but did rescue SJS-2W, a chromosomal knockout of *lpxA*. The complementation of the *lpxA::kan* mutant clearly shows that *AtlpxA* can functionally replace *EclpxA* despite the fact that SM101 was not complemented by *AtlpxA*. Perhaps the LpxA trimers formed from the mutant EcLpxA and AtLpxA do not possess sufficient catalytic activity to support growth. This chromosomal knockout of *lpxA* will serve as a valuable tool for studying the functions of other LpxA orthologs.

Our 2.1 Å resolution crystal structure of AtLpxA shows both conservation and variation of the LpxA structure. At first glance, the overall structure of AtLpxA is similar to the structure of EcLpxA. The conserved residues in AtLpxA align strikingly well with the active site residues of EcLpxA (Figure 6), when superimposed with EcLpxA complexed with the product UDP-3-*O*-[(*R*)-3-hydroxymyristoyl]-GlcNAc (PDB entry 2QIA).[11] All the residues important for catalysis of EcLpxA[11,15] are well conserved in AtLpxA. His180 (His125 in EcLpxA) is proposed to be a catalytic base, activating the GlcNAc 3-OH group to aid in the transfer of the acyl chain from (*R*)-3-hydroxymyristoyl-ACP,

and His199 (His144 in EcLpxA) is proposed to hydrogen bond with the GlcNAc 6-OH group of the substrate.[11,15]

As described above, the structure of AtLpxA supports the preference for a hydroxyacyl chain over an acyl chain. Gly173 in EcLpxA is well characterized as a hydrocarbon ruler,[11,14] allowing a longer hydroxymyristoyl chain in the active site as compared to the hydroxydecanoyl chain allowed by Met169-containing *Pseudomonas aeruginosa* LpxA. Gly228 in AtLpxA is analogous to Gly173 in EcLpxA. The presence of a small residue in this position supports the hydroxymyristoyl acyl chain selectivity suggested by the in vitro and in vivo data presented here.

While there are striking similarities between the EcLpxA and AtLpxA structures, several differences are worth noting. Initial alignment of the EcLpxA and AtLpxA sequences predicted two additional loops (Figure S1A of the Supporting Information). The longer 18-amino acid insert does not form a loop but instead forms three additional hexapeptide repeats. The initial sequence alignment did not recognize three of the hexapeptide repeats, [STAV]-X-[LIV]-[GAED]-X_2,[38] because of the presence of aromatic residues (Tyr and Phe) in the position usually occupied by small or negatively charged residues (Gly, Ala, Glu, and Asp). It is not clear whether AtLpxA has a complete coil C0 of 18 amino acids, as the eight amino-terminal residues (DSRDSE) did not show sufficient electron density. While the DSRDSE sequence is recognized as a hexapeptide repeat in sequence alignment using ClustalW, we suspect this region is rather unstructured. This additional coil, regardless of whether it is complete, is a significant difference between AtLpxA and other LpxA bacterial orthologs. Moreover, this additional coil does not appear to be unique to the *Arabidopsis* enzyme, as a sequence search finds other plant LβH proteins with additional hexapeptide repeats. For example, a putative LβH protein from *Populus trichocarpa* (NCBI entry XP_002308293.1) has three additional hexpeptide repeats probably forming a complete coil of C0, resulting in an LβH of 11 coils. The longest LβH domain reported so far exists in *E. coli* *N*-acetylglucosamine-1-phosphate uridyltransferase (GlmU) with 11 coils.[39] The functional consequence of this additional coil or the question of whether this extra coil is essential has yet to be addressed.

AtLpxA also has an additional four-amino acid loop, loop 0 (Glu104 to inserted Gly107), after coil C3. The OE1 atom of Glu104 in loop 0 is approximately 4 Å from the hydroxyl oxygen of Tyr78 from the adjacent monomer, possibly strengthening the interchain interaction. While this additional loop 0 does not appear to be present in the bacterial LpxA species, it exists in other plant LpxA species, suggesting an important structural role in these enzymes. Interestingly, the alignment of the AtLpxA and EcLpxA structures is better (rmsd of 0.8 Å with 170 Cα atom pairs) when the amino-terminal region of AtLpxA up to loop 0 is removed. This is likely due to the fact that the LβH domain of AtLpxA is bent around the loop 0 region toward turn 2 between sheets 2 and 3 by ~7° (Figure S4 of the Supporting Information). Among the LpxA protein structures reported so far, this bent rod shape for the LβH is seen only in AtLpxA and may be related to the presence of loop 0.

In conclusion, we have firmly established that AtLpxA is a functional LpxA through in vitro and in vivo analyses of its biochemical activity. While AtLpxA is structurally similar to EcLpxA, the differences between these structures may help illuminate the biological role of this protein and lipid A-like molecules in plants.

■ ASSOCIATED CONTENT

Supporting Information

Figures showing the sequence alignment of EcLpxA and AtLpxA (Figure S1), the overexpression and purification of AtLpxA (Figure S2), the scheme for the construction of Δ*lpxA E. coli* (Figure S3), and the bent rod shape of the LβH domain of AtLpxA (Figure S4). This material is available free of charge via the Internet at http://pubs.acs.org.

■ AUTHOR INFORMATION

Corresponding Author

*Phone: (845) 437-5738. Fax: (845) 437-5732. E-mail: tegarrett@vassar.edu.

Funding

This research was supported by National Institutes of Health Grant GM-51310 to C.R.H.R. and a National Research Foundation of Korea grant funded by the Korea government (MEST) to S.H.J. (2010-0003008).

Notes

The authors declare no competing financial interest.

■ ACKNOWLEDGMENTS

We thank Dr. Nathan Nicely and Mr. Chuljin Lee for assistance with X-ray diffraction experiments and Dr. Jinshi Zhao for assistance constructing the bacterial knockout strains. We thank Dr. Charles W. Pemble, IV, for his critical reading of the manuscript. Diffraction data were collected at Southeastern Regional Collaborative Access Team (SER-CAT) beamline 22-BM at the Advanced Photon Source, Argonne National Laboratory. Supporting institutions may be found at http://www.ser-cat.org/members.html. Use of the Advanced Photon Source, an Office of Science User Facility operated for the U.S. Department of Energy (DOE), Office of Science, by Argonne National Laboratory, was supported by the U.S. DOE under Contract W-31-109-Eng-38.

■ ABBREVIATIONS

ACP, acyl carrier protein; EcLpxA, *E. coli* LpxA; AtLpxA, *A. thaliana* LpxA; HpLpxA, *H. pylori* LpxA; LβH, left-handed parallel β-helix; LPS, lipopolysaccharide; ESI-MS, electrospray ionization quadrupole time-of-flight mass spectrometry; PBS, phosphate-buffered saline; UDP-GlcNAc, UDP-*N*-acetylglucosamine; LB, Luria-Bertani; TLSMD, Translation/Libration/Screw Motion Determination; rmsd, root-mean-square deviation; Hepes, 4-(2-hydroxyethyl)piperazine-1-ethanesulfonic acid; Kdo, 3-deoxy-D-*manno*-oct-2-ulosonic acid; PCR, polymerase chain reaction; SDS−PAGE, sodium dodecyl sulfate−polyacrylamide gel electrophoresis; ara, arabinose; cam, chloramphenicol; kan, kanamycin.

■ REFERENCES

(1) Raetz, C., Reynolds, C., Trent, M., and Bishop, R. (2007) Lipid A modification systems in Gram-negative bacteria. *Annu. Rev. Biochem.* 76, 295−329.

(2) Li, C., Guan, Z., Liu, D., and Raetz, C. R. (2011) Pathway for lipid A biosynthesis in *Arabidopsis thaliana* resembling that of *Escherichia coli*. *Proc. Natl. Acad. Sci. U.S.A. 108*, 11387−11392.

(3) Raetz, C., and Whitfield, C. (2002) Lipopolysaccharide endotoxins. *Annu. Rev. Biochem. 71*, 635−700.

(4) Galloway, S. M., and Raetz, C. R. (1990) A mutant of *Escherichia coli* defective in the first step of endotoxin biosynthesis. *J. Biol. Chem. 265*, 6394−6402.

(5) Anderson, M. S., and Raetz, C. R. (1987) Biosynthesis of lipid A precursors in *Escherichia coli*. A cytoplasmic acyltransferase that converts UDP-*N*-acetylglucosamine to UDP-3-*O*-(*R*-3-hydroxymyristoyl)-*N*-acetylglucosamine. *J. Biol. Chem. 262*, 5159−5169.
(6) Sweet, C., Lin, S., Cotter, R., and Raetz, C. (2001) A *Chlamydia trachomatis* UDP-*N*-acetylglucosamine acyltransferase selective for myristoyl-acyl carrier protein. Expression in *Escherichia coli* and formation of hybrid lipid A species. *J. Biol. Chem. 276*, 19565−19574.
(7) Lee, B. I., and Suh, S. W. (2003) Crystal structure of UDP-*N*-acetylglucosamine acyltransferase from *Helicobacter pylori*. *Proteins 53*, 772−774.
(8) Robins, L. I., Williams, A. H., and Raetz, C. R. (2009) Structural basis for the sugar nucleotide and acyl-chain selectivity of *Leptospira interrogans* LpxA. *Biochemistry 48*, 6191−6201.
(9) Chenna, R., Sugawara, H., Koike, T., Lopez, R., Gibson, T. J., Higgins, D. G., and Thompson, J. D. (2003) Multiple sequence alignment with the Clustal series of programs. *Nucleic Acids Res. 31*, 3497−3500.
(10) Raetz, C., and Roderick, S. (1995) A left-handed parallel β helix in the structure of UDP-*N*-acetylglucosamine acyltransferase. *Science 270*, 997−1000.
(11) Williams, A., and Raetz, C. (2007) Structural basis for the acyl chain selectivity and mechanism of UDP-*N*-acetylglucosamine acyltransferase. *Proc. Natl. Acad. Sci. U.S.A. 104*, 13543−13550.
(12) Claros, M. G., and Vincens, P. (1996) Computational method to predict mitochondrially imported proteins and their targeting sequences. *Eur. J. Biochem. 241*, 779−786.
(13) Guzman, L. M., Belin, D., Carson, M. J., and Beckwith, J. (1995) Tight regulation, modulation, and high-level expression by vectors containing the arabinose PBAD promoter. *J. Bacteriol. 177*, 4121−4130.
(14) Wyckoff, T., Lin, S., Cotter, R., Dotson, G., and Raetz, C. (1998) Hydrocarbon rulers in UDP-*N*-acetylglucosamine acyltransferases. *J. Biol. Chem. 273*, 32369−32372.
(15) Wyckoff, T., and Raetz, C. (1999) The active site of *Escherichia coli* UDP-*N*-acetylglucosamine acyltransferase. Chemical modification and site-directed mutagenesis. *J. Biol. Chem. 274*, 27047−27055.
(16) Miroux, B., and Walker, J. E. (1996) Over-production of proteins in *Escherichia coli*: Mutant hosts that allow synthesis of some membrane proteins and globular proteins at high levels. *J. Mol. Biol. 260*, 289−298.
(17) Bertani, G. (1951) Studies on lysogenesis. I. The mode of phage liberation by lysogenic *Escherichia coli*. *J. Bacteriol. 62*, 293−300.
(18) Bartling, C. M., and Raetz, C. R. (2008) Steady-state kinetics and mechanism of LpxD, the *N*-acyltransferase of lipid A biosynthesis. *Biochemistry 47*, 5290−5302.
(19) Bartling, C. M., and Raetz, C. R. (2009) Crystal structure and acyl chain selectivity of *Escherichia coli* LpxD, the *N*-acyltransferase of lipid A biosynthesis. *Biochemistry 48*, 8672−8683.
(20) Yu, D., Ellis, H. M., Lee, E.-C., Jenkins, N. A., Copeland, N. G., and Court, D. L. (2000) An efficient recombination system for chromosome engineering in *Escherichia coli*. *Proc. Natl. Acad. Sci. U.S.A. 97*, 5978−5983.
(21) Sambrook, J. G., and Russel, D. W. (2001) *Molecular Cloning: A Laboratory Manual*, 3rd ed., Cold Spring Harbor Laboratory Press, Plainview, NY.
(22) Bligh, E. G., and Dyer, W. J. (1959) A rapid method of total lipid extraction and purification. *Can. J. Biochem. Physiol. 37*, 911−917.
(23) Zhou, Z., White, K., Polissi, A., Georgopoulos, C., and Raetz, C. (1998) Function of *Escherichia coli* MsbA, an essential ABC family transporter, in lipid A and phospholipid biosynthesis. *J. Biol. Chem. 273*, 12466−12475.
(24) Raetz, C. R. H., Garrett, T. A., Reynolds, C. M., Shaw, W. A., Moore, J. D., Smith, D. C., Ribeiro, A. A., Murphy, R. C., Ulevitch, R. J., Fearns, C., Reichart, D., Glass, C. K., Benner, C., Subramaniam, S., Harkewicz, R., Bowers-Gentry, R. C., Buczynski, M. W., Cooper, J. A., Deems, R. A., and Dennis, E. A. (2006) Kdo_2-Lipid A of *Escherichia coli*, a defined endotoxin that activates macrophages via TLR-4. *J. Lipid Res. 47*, 1097−1111.
(25) Wang, X., Ribeiro, A., Guan, Z., Abraham, S., and Raetz, C. (2007) Attenuated virulence of a *Francisella* mutant lacking the lipid A 4′-phosphatase. *Proc. Natl. Acad. Sci. U.S.A. 104*, 4136−4141.
(26) Otwinowski, Z., and Minor, W. (1997) Processing of X-ray diffraction data collected in oscillation mode. In *Methods in Enzymology* (Carter, W. C., Jr., Ed.) pp 307−326, Academic Press, San Diego.
(27) McCoy, A. J., Grosse-Kunstleve, R. W., Adams, P. D., Winn, M. D., Storoni, L. C., and Read, R. J. (2007) Phaser crystallographic software. *J. Appl. Crystallogr. 40*, 658−674.
(28) McCoy, A. J., Grosse-Kunstleve, R. W., Storoni, L. C., and Read, R. J. (2005) Likelihood-enhanced fast translation functions. *Acta Crystallogr. D61*, 458−464.
(29) Emsley, P., and Cowtan, K. (2004) Coot: Model-building tools for molecular graphics. *Acta Crystallogr. D60*, 2126−2132.
(30) Murshudov, G. N., Vagin, A. A., and Dodson, E. J. (1997) Refinement of macromolecular structures by the maximum-likelihood method. *Acta Crystallogr. D53*, 240−255.
(31) Collaborative Computational Project, Number 4 (1994) The CCP4 suite: Programs for protein crystallography. *Acta Crystallogr. D50*, 760−763.
(32) Painter, J., and Merritt, E. A. (2006) Optimal description of a protein structure in terms of multiple groups undergoing TLS motion. *Acta Crystallogr. D62*, 439−450.
(33) Davis, I. W., Leaver-Fay, A., Chen, V. B., Block, J. N., Kapral, G. J., Wang, X., Murray, L. W., Arendall, W. B., Snoeyink, J., Richardson, J. S., and Richardson, D. C. (2007) MolProbity: All-atom contacts and structure validation for proteins and nucleic acids. *Nucleic Acids Res. 35*, W375−W383.
(34) Frishman, D., and Argos, P. (1995) Knowledge-based protein secondary structure assignment. *Proteins: Struct., Funct., Bioinf. 23*, 566−579.
(35) *The PyMOL Molecular Graphics System*, version 1.3r1 (2010) Schrodinger, LLC, New York.
(36) Crowell, D. N., Anderson, M. S., and Raetz, C. R. (1986) Molecular cloning of the genes for lipid A disaccharide synthase and UDP-*N*-acetylglucosamine acyltransferase in *Escherichia coli*. *J. Bacteriol. 168*, 152−159.
(37) Odegaard, T., Kaltashov, I., Cotter, R., Steeghs, L., van der Ley, P., Khan, S., Maskell, D., and Raetz, C. (1997) Shortened hydroxyacyl chains on lipid A of *Escherichia coli* cells expressing a foreign UDP-*N*-acetylglucosamine *O*-acyltransferase. *J. Biol. Chem. 272*, 19688−19696.
(38) Yoder, M. D., Keen, N. T., and Jurnak, F. (1993) New domain motif: The structure of pectate lyase C, a secreted plant virulence factor. *Science 260*, 1503−1507.
(39) Olsen, L. R., and Roderick, S. L. (2001) Structure of the *Escherichia coli* GlmU pyrophosphorylase and acetyltransferase active sites. *Biochemistry 40*, 1913−1921.